Civil Engineering Infrastructures Journal, 50(2): 293 – 310, December 2017
Print ISSN: 2322-2093; Online ISSN: 2423-6691
DOI: 10.7508/ceij.2017.02.006

A Finite Volume Formulation for the Elasto-Plastic Analysis of Rectangular Mindlin-Reissner Plates, a Non-Layered Approach

Fallah, N.[1*], Parayandeh Shahrestany, A.[2] and Golkoubi, H.[2]

[1] Associate Professor, Department of Civil Engineering, University of Guilan, Rasht, Iran and Associate Professor, Faculty of Civil Engineering, Babol Noshirvani University of Technology, Babol, Iran.
[2] M.Sc., Department of Civil Engineering, University of Guilan, Rasht, Iran.

Received: 27 Nov. 2016; Revised: 01 Aug. 2017; Accepted: 11 Aug. 2017

ABSTRACT: This paper extends the previous work of authors and presents a non-layered Finite Volume formulation for the elasto-plastic analysis of Mindlin-Reissner plates. The incremental algorithm of the elasto-plastic solution procedure is shown in detail. The performance of the formulation is examined by analyzing of plates with different boundary conditions and loading types. The results are illustrated and compared with the predictions of the layered approach. These several comparisons reveal that the non-layered Finite Volume approach can present accurate results with low CPU time usage despite its simplicity of the solution procedure.

Keywords: Elasto-Plastic, Finite Volume, Layered Approach, Mindlin Plate, Non-Layered Approach.

INTRODUCTION

The bending theory of plates has been established during the past decades. Classic plate theory (Timoshenko and Woinowsky, 1970), first order shear deformation theory (Reissner, 1945) and higher order shear deformation theory (Reddy, 2004) are some of them. The first order shear deformation theory of plate, also known as Mindlin-Reissner theory, has been preferred in numerical modeling. For example, Finite Element analysis of thin to the moderately thick plates, which due to C^o continuity requirement for the displacement, can be attained with ease (Owen and Hinton, 1980; Sudhir, 2012; Rezaiee-Pajand and Sadeghi, 2013). However, it should be mentioned that in the case of very thin plate analysis, the Mindlin-Reissner based Finite Element formulation suffers from shear locking deficiency. So it needs special techniques such as reduced integration (Prathap and Bhashyam, 1982) and selective integration (Hughes et al., 1978). Behavior of plates has been analyzed by other numerical methods such as the finite strip (Mirzaei et al., 2015), element free Galerkin (Naderi and Baradaran, 2013; Edalati and Soltani, 2015; Mikaeeli and Behjat, 2016), meshless based methods (Liu, 2010) and other works (Kim et al., 2009; Osadebe and Aginam, 2011; Ruocco and Fraldi, 2012; Xu and Zhou, 2010; Ghannadiasl and Noorzad, 2016; Mirzapour et al., 2012; Shahabian et al., 2013). Although Finite Volume technique

* Corresponding author E-mail: fallah@guilan.ac.ir; fallah@nit.ac.ir

is rather a new arrival as a numerical method for the solution of solid mechanics problems compared to the Finite Element method, however, it has shown promising capabilities in studies so far. Elastic analysis of three-dimensional solids (Bailey and Cross, 1995), stress analysis of elasto-plastic solids (Demirdzic and Martinovic, 1993), FV methods for different solid mechanics problems (Cardiff et al., 2017; Cardiff et al., 2016; Aguirre et al., 2015; Tang et al., 2015; Nordbotten, 2014; Trangenstein, 1991; Demirdzˇic´ et al., 1988), FV-based flow formulations to simulate plastic deformation processes (Basic´ et al., 2005; Trangenstein, 1991), bending analysis of elastic plates (Wheel, 1997; Fallah, 2004; Fallah, 2006), Finite Volume analysis of dynamic fracture problems (Ivankovic et al., 1994; Stylianou and Ivankovic, 2002) and studying periodic and functionally graded media (Cavalcante et al., 2011; Cavalcante et al., 2012; Cavalcante and Pindera, 2012) are some of the works which have highlighted notable capabilities of the Finite Volume method.

This paper extends the present author's work on the application of Finite Volume method for the elasto-plastic analysis of Mindlin plates in which the layered approach was adopted (Fallah and Parayandeh, 2014). There is another method for the numerical analysis of Mindlin plates known as the non-layered approach which involves fewer computations compared to the layered approach. In a layered approach, the plate thickness is divided into some layers, and the stress at the middle of each layer represents the stress value of the layer. According to the equivalent stress value of each layer, it is concluded whether the layer is in the elastic state or plastic state. The non-layered approach works with the stress resultants and determines the elastic or plastic state of any point of the plate by evaluating the bending moment components. In the non-layered approach, it is assumed that each plate cross section enters instantaneously to the plastic state, while, in the layered approach, the cross section becomes gradually plastic by entering the layers to the plastic regime one by one. This gradual development of plasticity through the plate thickness results in smoother responses due to the increasing applied loads. This smooth transition from the elastic state to the fully plastic state can be seen in the load-displacement paths of the plates. Since the layered approach considers the evolution of plasticity over the plate thickness, it can provide more realistic information of the plate plasticization than the non-layered approach.

In this work, a Finite Volume based formulation is presented for bending analysis of elasto-plastic Mindlin plates by adopting the non-layered model. After giving the Finite Volume formulation of the Mindlin plate, a discussion on the non-layered model is first provided (Harrison et al., 1984; Shi and Voyiadjis, 1992; Xia et al., 2011). Then, the layered model will be discussed briefly according to work (Fallah and Parayandeh, 2014). The novelty of this work lies in the presented development made in the Finite Volume method for the plastic analysis of plates using the non-layered approach which has not been presented so far. The shear effects have been considered in the formulation which provides the possibility of plastic analysis of both thin and moderately thick plates. As can be seen in the test results, both of the layered and non-layered approaches can do plastic analysis without any shear locking deficiency. In all the results presented in this work, it has been demonstrated that the non-layered approach can present accurate results with low CPU time usage despite its simplicity of the solution procedure.

The outline of the present paper is as follows: after introduction, elasto-plastic formulations of the plates are presented. Then, the cell-centered Finite Volume technique is provided for obtaining the discretized system equation using the non-layered model of the elasto-plastic plate. Afterwards, the solution procedure is given, and then the numerical studies of some test problems are presented. Finally, we prepared the conclusions.

ELASTO-PLASTIC FORMULATION OF MINDLIN-REISSNER PLATES

By applying the Mindlin–Reissner assumptions and small displacement plate bending theory, the displacement components of a point of coordinates x, y, z are:

$$\begin{aligned} u &= z\,\beta_x\,(x,y) \\ v &= z\,\beta_y\,(x,y) \\ w &= w(x,y) \end{aligned} \tag{1}$$

where w: is the transverse displacement, β_x and β_y: are the rotations of the plate section in the xz and yz planes, respectively. Figure 1 shows the sign convention used for the above displacement components.

There are two approaches for the elasto-plastic analysis of plates which are the layered approach and the non-layered approach. In the layered approach, which is able to capture the spread of plasticity over the plate thickness, the plate is divided into some layers. Each layer may become plastic separately. As the number of layers increases, this model provides a more realistic representation of the gradual spread of plasticity over the plate cross-section. In the non-layered approach, when the bending moment at any location of the plate reaches the yield moment, it is assumed that the entire thickness of the plate becomes plastic instantaneously. In this paper, we deal with the Finite Volume analysis of the non-layered approach. The Finite Volume analysis of layered approach has been discussed in Fallah and Parayandeh (2014) in detail.

As mentioned above, in non-layered approach, the entire cross-section becomes plastic when the bending moment reaches the yield value ($M_Y = \sigma_Y t^2/6$), where σ_Y: is the material uniaxial yield stress, t: is the plate thickness, and M_Y: is bending moment per unit of length.

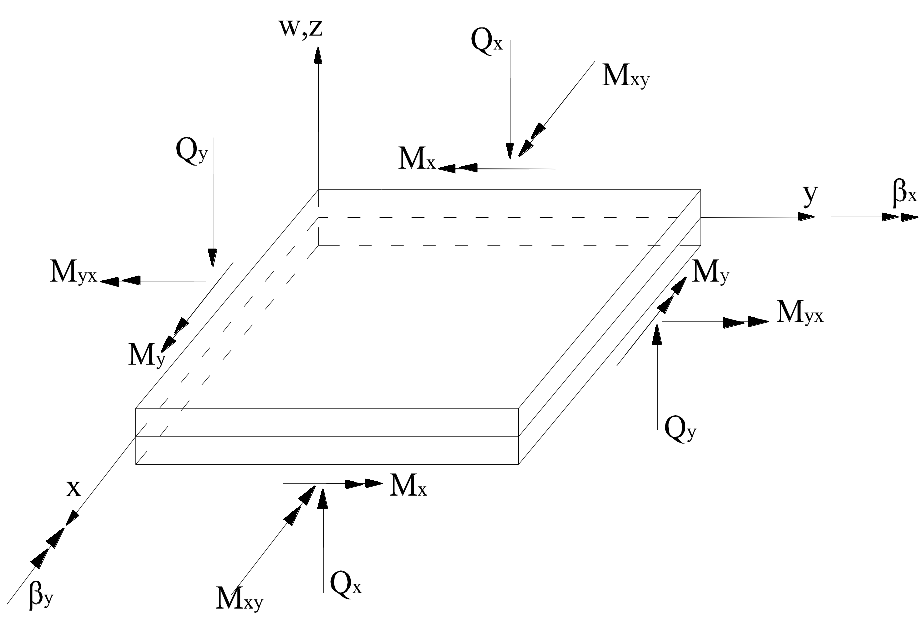

Fig. 1. Sign convention of the moment, shear force, and section rotation

The stress-strain relation for the plate with plastic deformation has the following form:

$$ds^f = D_{ep} d\varepsilon \tag{2}$$

where ds^f : is bending moment increment, $d\varepsilon$: is flexural strain increment and D_{ep} : is plastic stress-strain matrix which is the modified elastic flexural rigidity of plate due to the plasticization.

For Mindlin plates, it is assumed that the yield function *F*: is a function of the bending moments vector, s^f , but not of the transverse shear forces, s^s . The yield function is also a function of the hardening parameter *h.* The yield function *F* can be expressed as

$$F(s^f, h) = f(s^f) - M_Y(h) \tag{3}$$

where

$$f(s^f) = M_{von} = (M_x^2 + M_y^2 - M_x M_y + 3M_{xy}^2)^{1/2} \tag{4}$$

when yielding occurs, it is assumed that the stress resultants must remain on the yield surface so that

$$F(s^f, h) = f(s^f) - M_Y(h) = 0 \tag{5}$$

To explain the elasto-plastic constitutive equations of the plate, the following calculations are performed which can be found in Owen and Hinton (1980). By differentiating of Eq. (5) we have

$$dF = \frac{\partial F}{\partial s^f} ds^f + \frac{\partial F}{\partial h} dh = 0 \tag{6}$$

The incremental relationship between the generalized stress and generalized strain for the elasto-plastic deformation is

$$d\varepsilon = D^{-1} ds^f + a d\lambda \tag{7}$$

where $a^T = \partial F / \partial s^f$ known as the plastic flow vector of the plate, which the effect of Q_x and Q_y on the plastic behavior of plate is ignored. $d\lambda = (a^T D / A + a^T D a) d\varepsilon$ is also known as the plastic multiplier in which $A = (-1/d\lambda)(\partial F / \partial h) dh$ is the hardening parameter which depends on the hardening rule of the plate material. Multiplying both sides of Eq. (7) by $a^T D$ gives

$$a^T D d\varepsilon = a^T ds^f + a^T D a d\lambda \tag{8}$$

Using the above equation, one can obtain

$$ds^f = \left[D - \frac{D a a^T D}{A + a^T D a} \right] d\varepsilon \tag{9}$$

alternatively, in the compact form as presented in Eq. (2), we have $D_{ep} = D - (d_D d_D^T / A + d_D^T a)$ which $d_D = Da$.

DISCRETIZED SYSTEM EQUATION OF THE FINITE VOLUME METHOD FOR THE MINDLIN PLATE

Figure 2 shows a part of the mid-plane of a plate, which is meshed to some elements where each element is referred to as control volume or cell. A control volume is bounded by an arbitrary number of faces, and its center is considered as a computational node.

The equilibrium equations of a typical control volume *P* shown in Figure 2, can be represented by

$$\begin{cases} \sum_i^m M_x = 0 \\ \sum_i^m M_y = 0 \\ \sum_i^m F_z = 0 \end{cases} \tag{10}$$

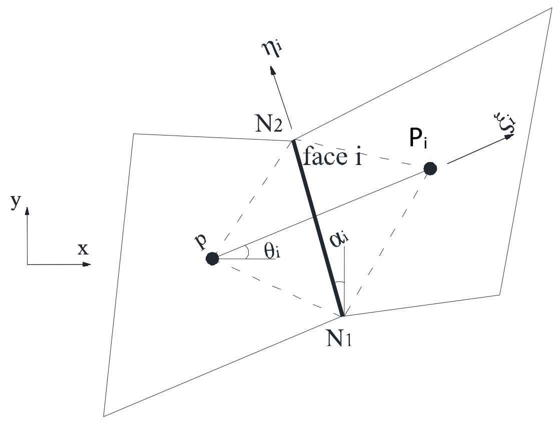

Fig. 2. Two adjacent control volumes on a mesh of elements

where the first two equation expresses the equilibrium of moments about the global *x* and *y* axes, respectively, and the last equation represents the equilibrium state in the *z* direction. By assuming a uniform distribution of moments and shear forces along the control volume faces, the above equilibrium equation may be rewritten as

$$\sum_{i=1}^{m}\left\{\begin{bmatrix} 0 & 0 & 0 \\ 0 & n_y^i & n_x^i \\ n_x^i & 0 & n_y^i \end{bmatrix}\begin{Bmatrix} M_x^i \\ M_y^i \\ M_{xy}^i \end{Bmatrix} - \begin{bmatrix} n_x^i & n_y^i \\ n_x^i (Y_i) & n_y^i (Y_i) \\ n_x^i (X_i) & n_y^i (X_i) \end{bmatrix}\begin{Bmatrix} Q_x^i \\ Q_y^i \end{Bmatrix}\right\}$$

$$L_i = \begin{Bmatrix} qA_p \\ 0 \\ 0 \end{Bmatrix} \quad (11)$$

where the illustrated sign convention of Figure 1 is used. For a given face i, n_x^i and n_y^i: are cosine direction of outward normal of face i, x_i and y_i: are the coordinate of midpoint of face i, x_p and y_p: are the coordinate of cell centre (computational point), q: is the uniformly distributed load applied upon the cell, A_p and L_i: are the mid-surface area of cell and the length of face i, M^i and Q^i: are moment and shear force correspond to the middle of face i, respectively which are measured per unit length (Fallah, 2004).

For a Mindlin plate, the incremental constitutive equation is given in the form of

$$\begin{Bmatrix} \Delta M_x \\ \Delta M_y \\ \Delta M_{xy} \end{Bmatrix} = \Delta(D^* \begin{Bmatrix} \dfrac{\partial \beta_x}{\partial x} \\ \dfrac{\partial \beta_y}{\partial y} \\ \dfrac{\partial \beta_x}{\partial y} + \dfrac{\partial \beta_y}{\partial x} \end{Bmatrix}) \, , \quad (12)$$

$$D^* = D\begin{bmatrix} 1 & \nu & 0 \\ \nu & 1 & 0 \\ 0 & 0 & \dfrac{1-\nu}{2} \end{bmatrix}$$

$$\begin{Bmatrix} \Delta Q_x \\ \Delta Q_y \end{Bmatrix} = \Delta(k_s G t \begin{Bmatrix} \dfrac{\partial w}{\partial x} + \beta_x \\ \dfrac{\partial w}{\partial y} + \beta_y \end{Bmatrix}) \quad (13)$$

where D^*: is the plate constitutive matrix, D: is the plate flexural rigidity, ν: is Poisson's ratio, k_s: is the lateral shear correction factor which is due to the assumption of constant transverse shear strains, G: is the shear modulus, and t: is plate thickness. In the case of the elastic state, $D = Et^3/12(1-\nu^2)$, however, for the plastic analysis, it is modified to D_{ep} as discussed before. The bending/twisting moments and shear forces corresponding to a face of a cell can be calculated when the derivatives of displacement components presented in Eqs. (12) and (13) are calculated on the global coordinates *xy*. These derivatives can be first approximated using the local coordinate axes $\xi\eta$ (see Figure 2) and then transformed to the global coordinate system *xy*. The details of the derivative calculations and explanations on Figures 2 and 3 have been given in Fallah (2004). By introducing the constitutive equations to the equilibrium Eq. (11) and some extra works on the resulted equation, the final set of the approximated equilibrium equations of a typical cell, *P*, can be expressed in the form of

$$k_P \begin{Bmatrix} \Delta\beta_x \\ \Delta\beta_y \\ \Delta w \end{Bmatrix}_P + \sum_{i=1}^{N} k_i \begin{Bmatrix} \Delta\beta_x \\ \Delta\beta_y \\ \Delta w \end{Bmatrix}_i = \Delta f \qquad (14)$$

where k_P and k_i : are matrix form and constant. They are dependent on the cell geometry and material properties. Their size is 3×3. *N*: represents the number of cells surrounding the cell, *P*. Also, vector $\Delta \boldsymbol{f}$ includes information of loads applied to the cell P.

Equation (14) describes the equilibrium of the cells in an approximate sense. For having a complete description of the plate equilibrium state, it is also needed to describe the boundary conditions of the plate. In general, there are three types of boundary conditions: essential boundary conditions, natural boundary conditions and a mixed kind of boundary conditions. To approximate the boundary conditions, a point cell is considered in the middle of the face lying on the plate boundary, corresponding to a cell adjacent to the plate boundary, Figure 3. Two equations corresponding to each point cell can be written which describes the point cell conditions according to the above three types of boundary conditions. These equations for all the point cells can be incorporated into equilibrium Eq. (14) which provides the whole system equations. The details of equations corresponding to the above three types of boundary conditions can be found in Fallah (2004, 2006).

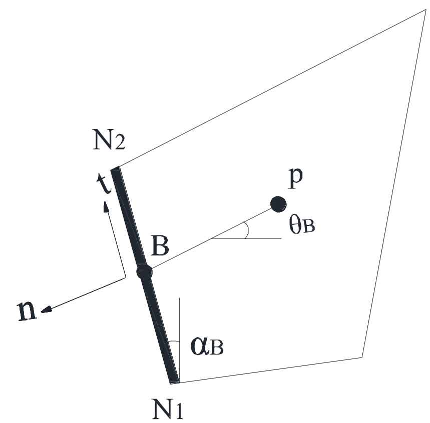

Fig. 3. A typical point cell

It should be noted that corresponding to each point cell, for the rotation about the normal vector of the boundary, two different situations are possible as hard boundary condition or soft boundary condition (Bathe, 1996). With considering *w* as the lateral displacement, β_t and β_n are section rotations at the boundary about normal vector, *n* and tangent vector, *t* of the boundary respectively, (see Figure 3). For simply supported plate, if one considers *w=0*; but β_t and β_n are free, the boundary condition is considered as soft type, however when β_t is also set to zero, the boundary condition is the hard type. On the other hand, when the plate edge is clamped, in the soft boundary condition, we have $w = \beta_n = 0$ and β_t is free, but in the hard boundary condition we also have $\beta_t = 0$. In this work we assume a hard, boundary condition type.

SOLUTION PROCEDURE

When mixed boundary conditions are applied, a proper combination of equations mentioned earlier should be used. According to the internal cells and boundary conditions equations, a system of simultaneous linear equations can be written, which relates the unknowns and could be expressed in the matrix form. It is evident that due to the existence of nonlinearity of material, the plate is analyzed step by step corresponding to the load increments. However, the whole system equations can be stated as follows

$$K\,\Delta U = \Delta F \tag{15}$$

where matrix K: is the coefficients appeared in Eq. (14) and equations in the boundaries conditions. It should be noted that matrix K is un-symmetric, is not constant and its entries are changed by developing the plasticity in the plate. The vector ΔF contains the incremental loads and known values relevant to the boundary conditions. The governing Eq. (15) can be solved by a direct solver technique and each load increment results in the displacement increment (ΔU).

The solution algorithm for the elasto-plastic Finite Volume analysis of the Mindlin plates using the non-layered approach is presented in Figure 4 where i is the cell number and j is the face number of a considered cell.

As it can be seen above, corresponding to each load increment, first, the incremental displacement vector is calculated using Eq. (15). Then, for each cell's face of the domain, the incremental bending moments and shear forces are calculated using Eqs. (12) and (13). Then, the Von Mises or equivalent moment of the face, M_{von}, is calculated using Eq. (4). If the equivalent bending moment, M_{von}, is greater or equal to the yield moment M_y, the whole thickness of the plate corresponding to the considered face becomes or has already become plastic instantaneously. Subsequently the load scaling factor R is calculated. Finally, the stress should be reduced to the yield surface. It should be mentioned that instead of the above solution algorithm, the Newton-Raphson procedure can be used which has been applied in Fallah and Parayandeh (2014). However, the present method is easy to be implemented regarding the computer programming which is employed in this work The presented iteration method is independent of loading increment size, due to using the load scaling factor R. This method decreases the given load increment to a minimum size so that just one element, in the non-layered approach, or one layer, in the layered approach, is yielded corresponding to the scaled load increment. Hence, loading increment size is not important in the present procedure. On the other hand, the Newton-Raphson procedure is dependent to load increment size. Corresponding to a load increment, it is possible that some elements or some layers are yielded simultaneously. So, loading increment size is important, and if one applies a big load increment size, the procedure may not be able to reach to a converged state with ease.

NUMERICAL RESULTS

By using the above-presented procedures, the elasto-plastic bending of a square plate with unit side length and different types of loads and boundary conditions is investigated. The following geometric and material properties are used: t = 0.01 m, $k_s = \frac{5}{6}$, υ = 0.3, E = 200 GPa, $\sigma_Y = 250$ MPa. The hardening parameter A is chosen equal to zero which enables to perform the elastic perfectly plastic analysis. Corresponding to each case, the relevant graphs for the load-displacement path at the plate center, elastic-plastic bending moment and shear force across the plate's central cross-section are presented in the following subsections.

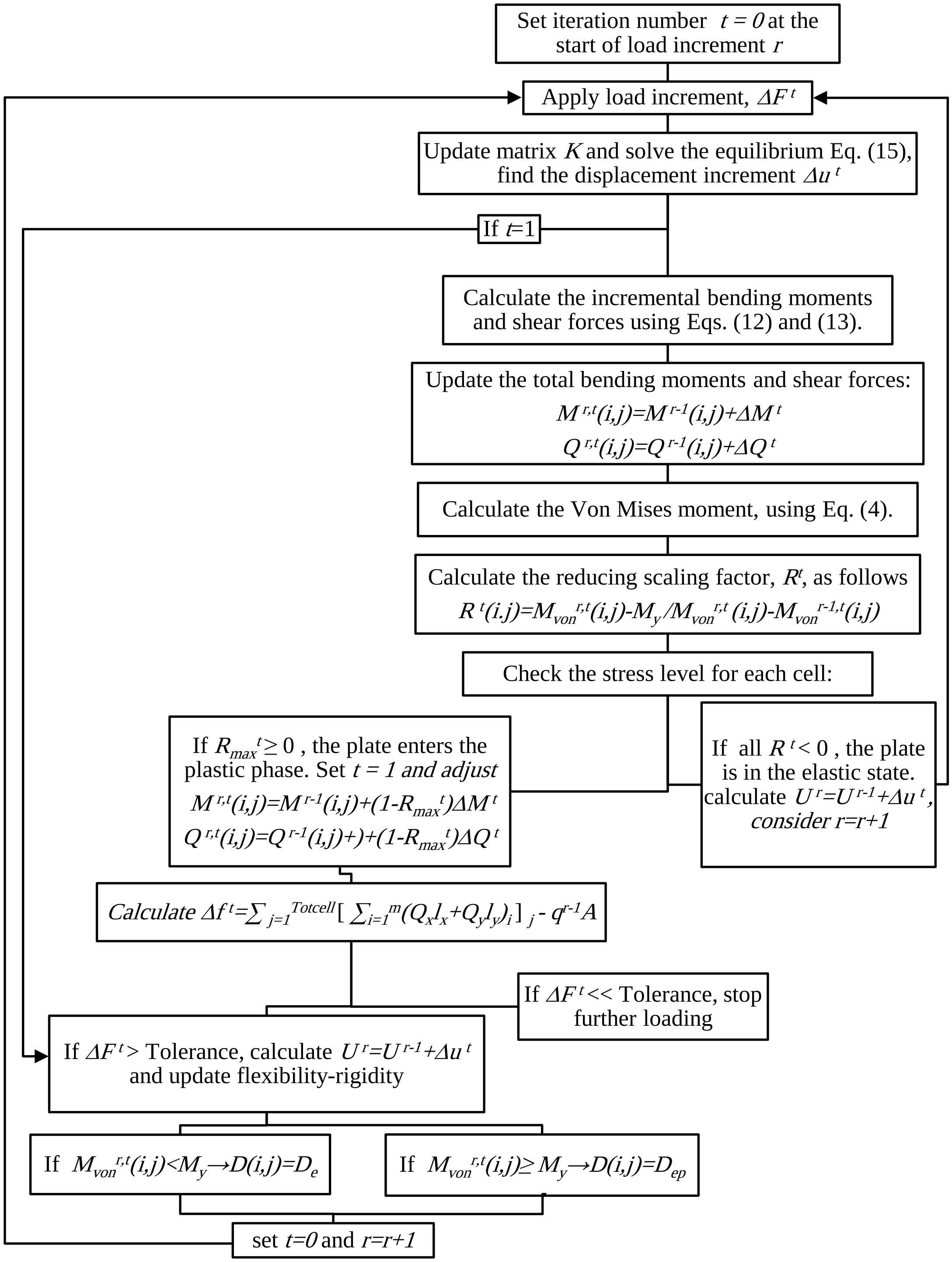

Fig. 4. The iterative solution procedure in non-layered approach for the elasto-plastic analysis of Mindlin plates, (*Note*: it is assumed that $H'=0$)

In some of the figures presented in this section, the dimensionless load parameter, PL^2/M_P , and the dimensionless plate center displacement, $wD/M_P L^2$, are used for the vertical and horizontal axes respectively. In above parameters, P is the uniform load intensity, $M_P=\sigma_Y t^2/4$ is the fully plastic moment per unit length of the plate cross-section, D: is plate elastic bending rigidity, L

is the plate side length and *w* is the plate center deflection.

Simply Supported Plate Subjected to a Uniformly Distributed Load

To demonstrate how the predictions of the non-layered approach are converged due to the grid refinement, a systematic grid refinement has been performed and the dimensionless plate center displacement, $wD/M_P L^2$, has been calculated corresponding to two load parameter values of $PL^2/M_P = 5$ and $PL^2/M_P = 20$. The convergence behavior of both non-layered and layered approaches can be seen in Figure 5 where ten layers are used for the layered approach. As can be seen, 7×7 divisions along the plate sides produces grid independent results corresponding to both load parameter values.

According to the above results, for obtaining the load-displacement path corresponding to the plate center, a mesh of 7×7 divisions for the non-layered and layered approaches with ten layers for the layered approach is used.

An initial load increment of 100 Pa is considered. The results corresponding to the load-displacement path of the plate center are obtained which is shown in Figure 6.

In Figure 6 the results of the present method are compared with the results of ANSYS software which is obtained by using element type of shell-181 with the capability of the layered model. The elasto-plastic analysis of the considered plate by ANSYS has shown that a mesh of 14×14 equal divisions with ten layers produces grid-independent results. It can be observed that the layered and non-layered methods predict the equilibrium path close to the prediction of the ANSYS. It is clear that the layered method is more accurate than the non-layered one. For comparing the simulation speed of both approaches, Figure 7 is given. As can be seen, the non-layered approach is much faster than the layered one.

In Figures 8 and 9 the results corresponding to bending moment and shear force, obtained by layered and non-layered approaches, are compared with each other. A plate cross section at *y* = 0.5 is considered. A good agreement can be seen between the results of bending moment and shear force predictions by two approaches. As it can be seen, while their shear force predictions are very close, there are some discrepancies in the predictions of bending moments, which is due to the considered load value of $PL^2/M_P = 20.7$. In Figure 5, it can be seen that corresponding to $PL^2/M_P = 20.7$, two approaches have different predictions, so it is expected that their bending moment predictions should be different too. In Figure 10 we used a lower load value, $PL^2/M_P = 16$, and it can be seen that the difference in the bending moment predictions is reduced. Also in Figure 10, we presented two sets of results corresponding to two thickness ratioes, L/t = 10 and 100. As can be seen, both layered and non-layered approaches are able to predict bending moments of thin and moderately thick plates.

Simply Supported Plate Subjected to a Concentrated Load at the Center

In this test, the loading upon the plate is considered as a concentrated load at the plate center. The plate is meshed to a number of elements in which the center of an element coincides with the plate center where the concentrated load is applied. The studies have shown that a mesh of 13×13 and ten layers produce converged results in a layered approach and a mesh of 13×13 for the non-layered approach, which are used in this part for the comparison purpose. Figure 11 shows the equilibrium paths obtained by the present method. Figures 12 and 13 illustrate a comparison between layered and non-layered predictions for the bending moment and shear force of plate cross section at y = 0.5.

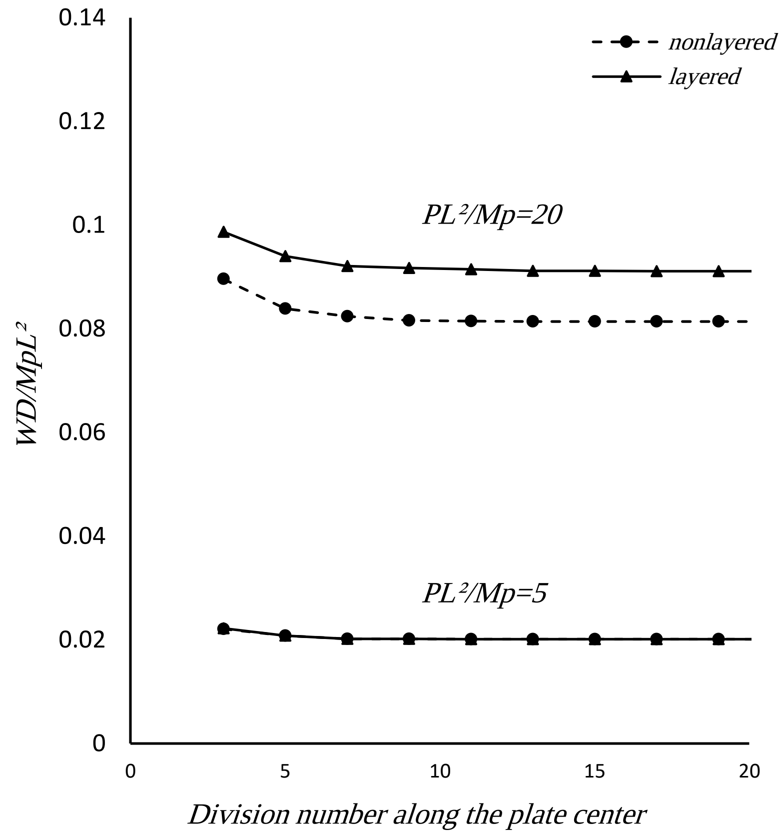

Fig. 5. Displacement at the plate center

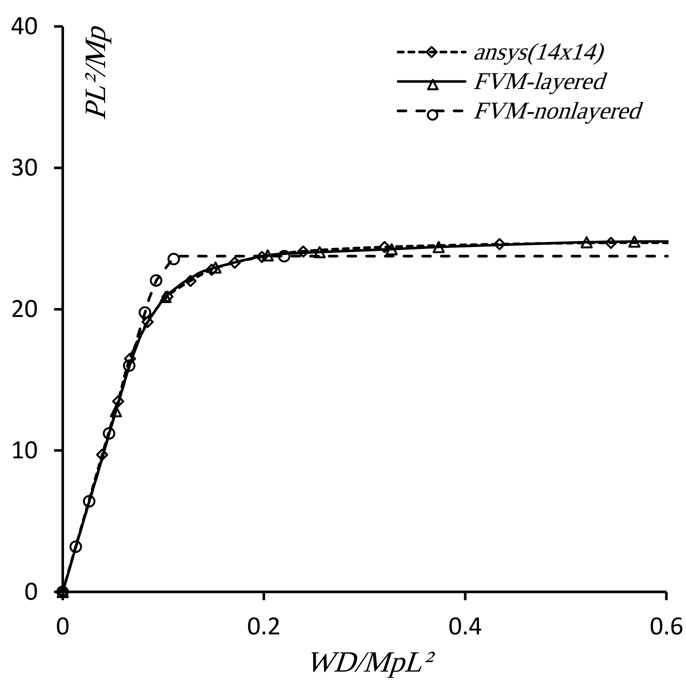

Fig. 6. Load-deflection paths obtained by layered and non-layered approaches for the simply supported plate subjected to a uniformly distributed load

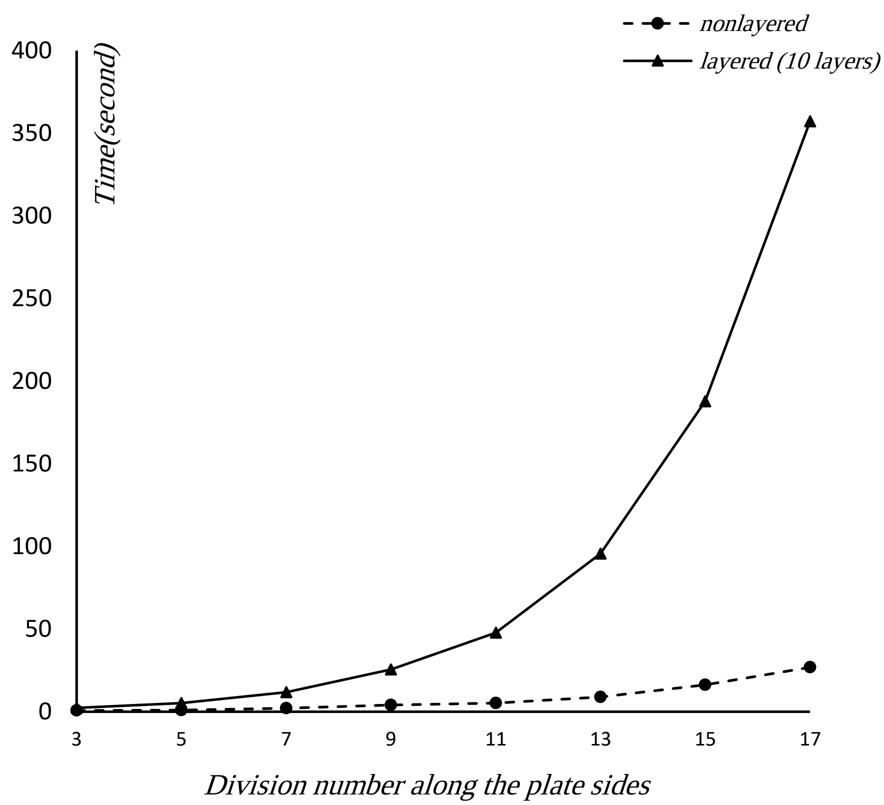

Fig. 7. CPU time usage of layered and non-layered approaches

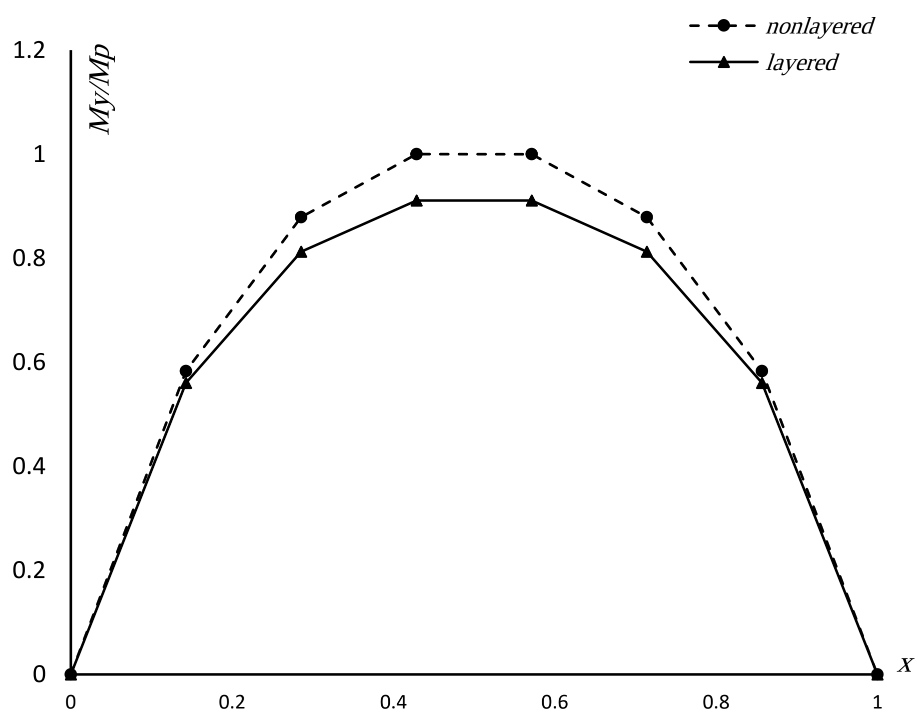

Fig. 8. Moment diagram at the middle cross section (y = 0.5) corresponding to $PL^2/M_P = 20.7$ (simply supported plate subjected to a uniformly distributed load)

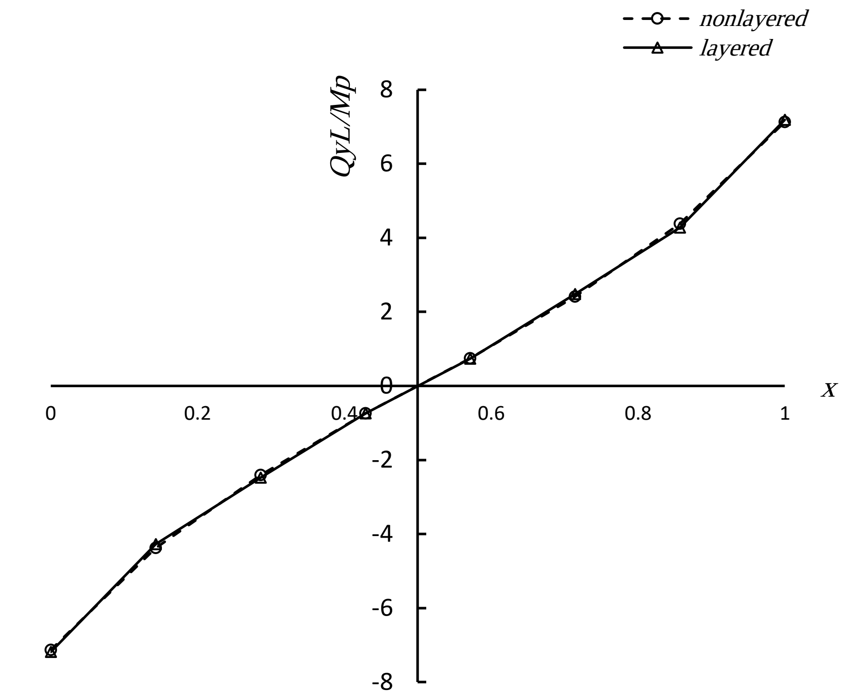

Fig. 9. Shear force diagram at the middle cross section (y = 0.5) corresponding to $PL^2/M_P = 20.7$ (simply supported plate subjected to a uniformly distributed load)

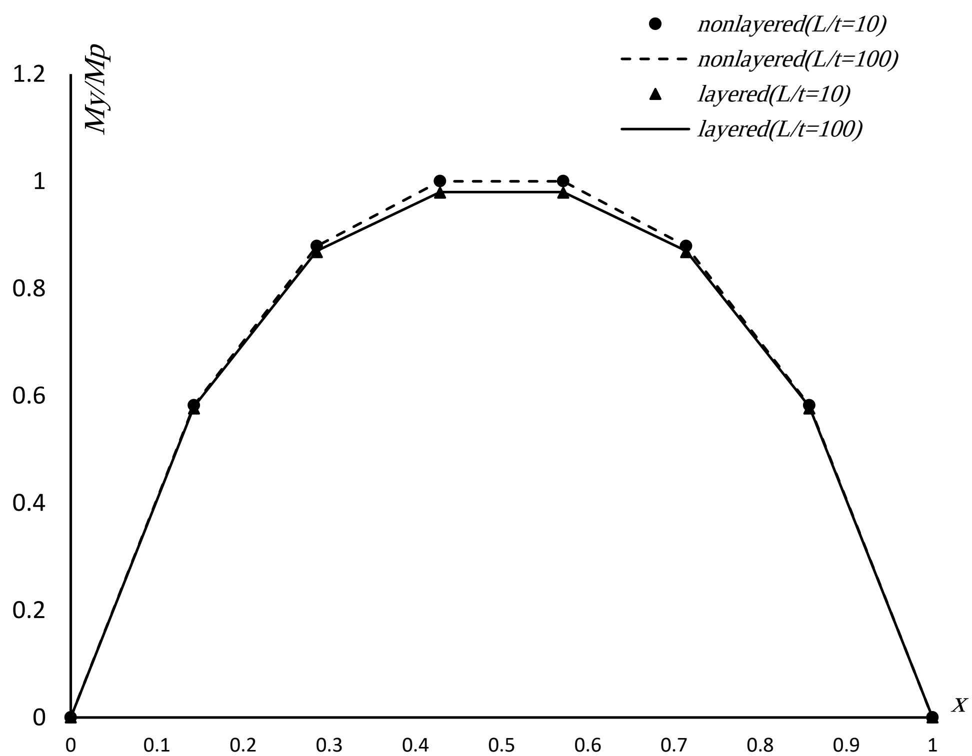

Fig. 10. Moment diagram at the middle cross section(y = 0.5) corresponding to $PL^2/M_P = 16$ and different *L/t* (simply supported plate subjected to a uniformly distributed load)

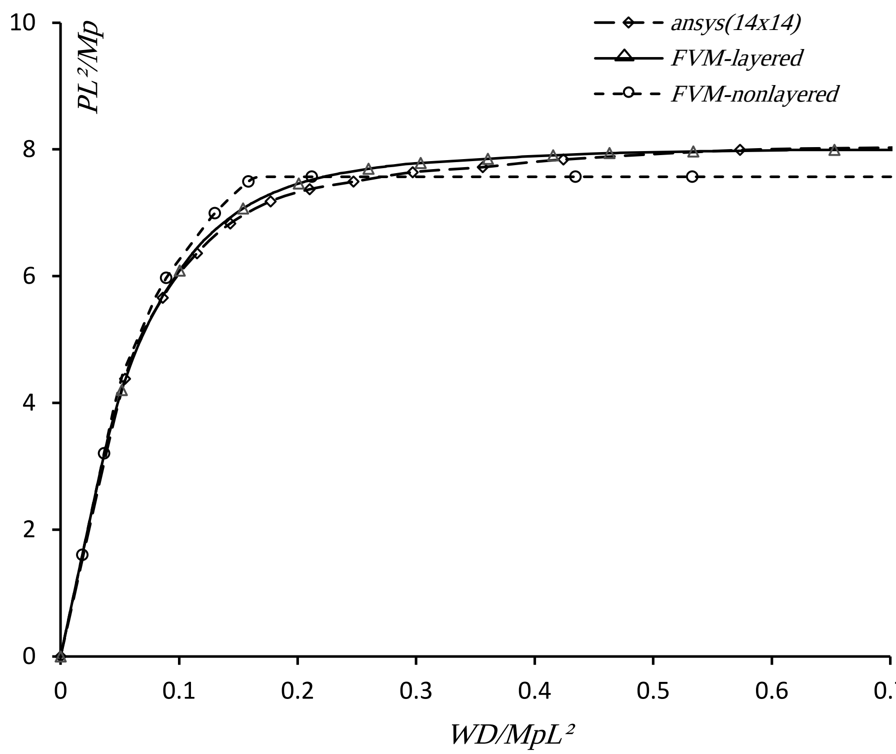

Fig. 11. Load-deflection paths obtained by layered and non-layered approaches for the simply supported plate subjected to a concentrated load at the center

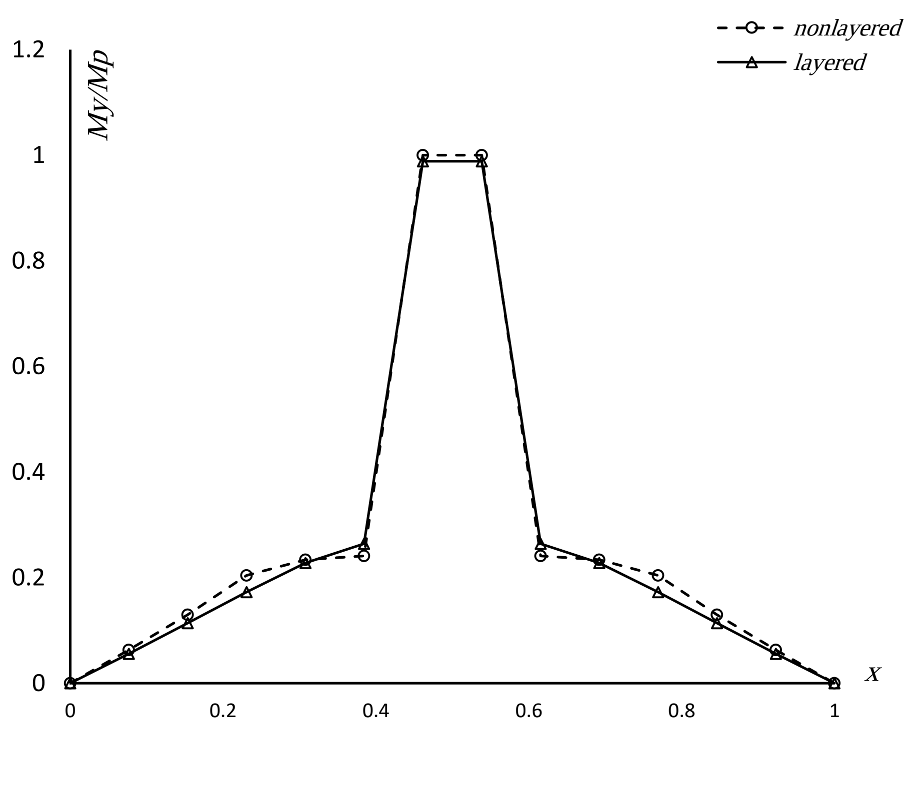

Fig. 12. Moment diagram at the middle cross section (y = 0.5) corresponding to $PL^2/M_P = 6.5$ (simply supported plate subjected to a concentrated load at the center)

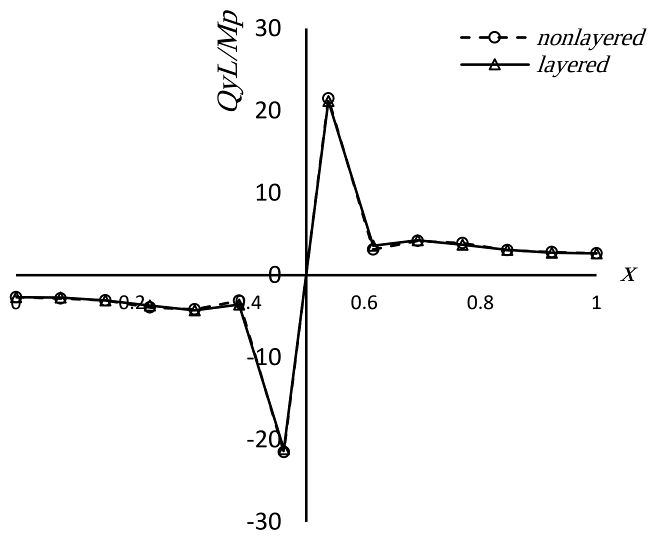

Fig. 13. Shear force diagram at the middle cross section (y = 0.5) corresponding to $PL^2/M_P = 6.5$ (simply supported plate subjected to a concentrated load at the center)

Clamped plate subjected to uniformly distributed load

The boundaries of the plate are changed to the clamped ones where the plate is under the uniformly distributed load. The studies have shown that a mesh of 15×15 with ten layers in a layered approach and a 15×15 mesh in non-layered approach produce converged results which are used in this part for the comparison purpose. Figure 14 shows the load-displacement paths obtained using the present methods. Comparison between the predictions of bending moment and shear force distributions at the cross section of $y = 0.5$ corresponding to $PL^2/M_P = 24$ are shown in Figures 15 and 16.

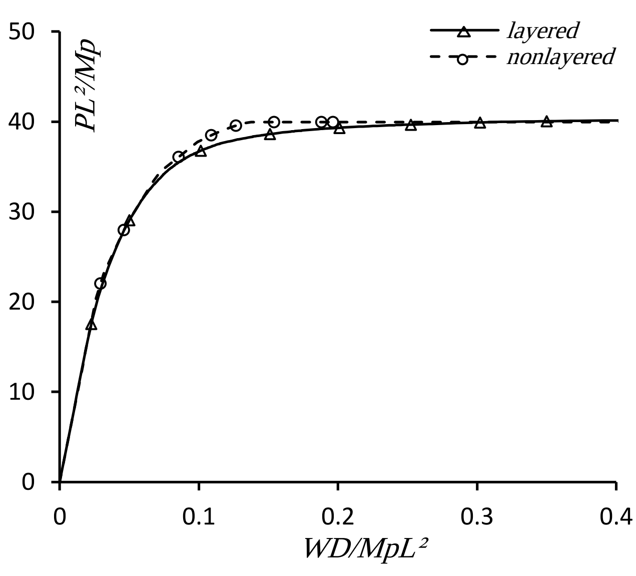

Fig. 14. Load-deflection paths obtained by layered and non-layered approaches for the clamped plate subjected to uniformly distributed load

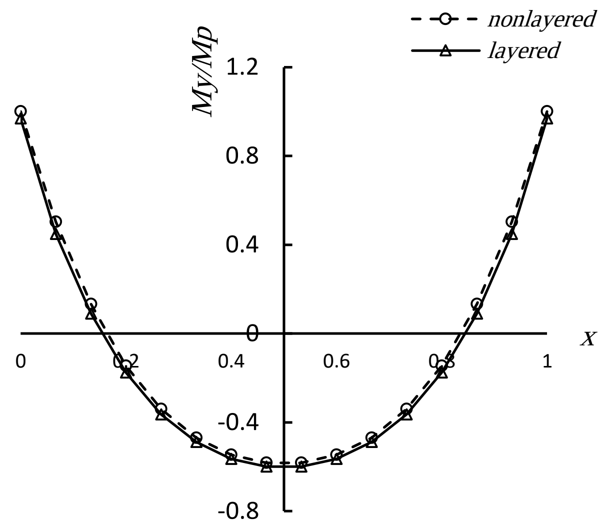

Fig. 15. Moment diagram at the middle cross section (y = 0.5) corresponding to $PL^2/M_P = 24$ (clamped plate subjected to uniformly distributed load)

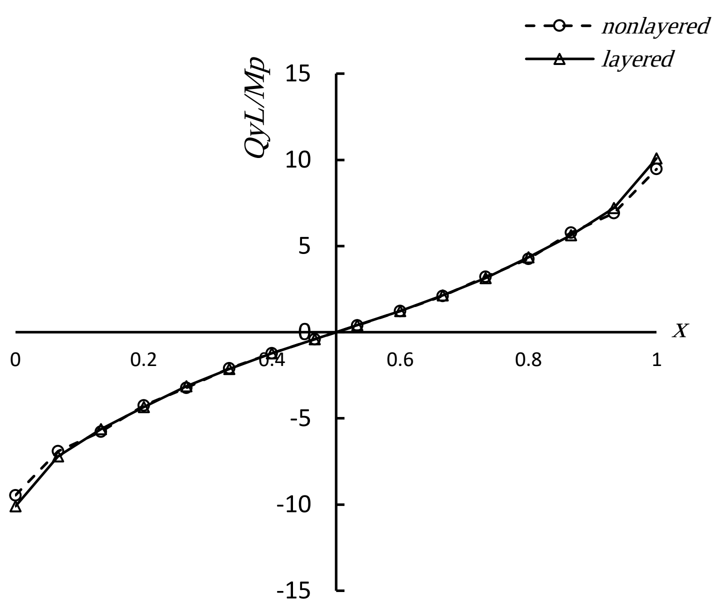

Fig. 16. Shear force diagram at the middle cross section (y = 0.5) corresponding to $PL^2/M_P = 24$ (clamped plate subjected to uniformly distributed load)

Also for performing a comprehensive study, the following boundary conditions and loading types have been studied for the considered plate:

- Plate with four edges clamped subjected to a concentrated load at the center.
- Plate with two opposite edges simply supported, and the other two edges clamped subjected to uniformly distributed the load.
- Plate with two opposite edges simply supported, and the other two edges clamped subjected to a concentrated load at the center.
- Plate with two opposite edges simply supported, and the other two edges free

subjected to uniformly distributed the load.

- Plate with two opposite edges simply supported and the other two free edges subjected to a concentrated load at the center
- Plate with two opposite edges clamped and the other two free subjected to uniformly distributed the load.
- Plate with two opposite edges clamped and the other two free subjected to a concentrated load at the center.

The elasto-plastic responses of the considered plate with the above boundary conditions and loading types have been studied, and the layered and non-layered approaches have shown almost similar performances as observed in Figsure 6 to 16.

CONCLUSIONS

A non-layered Finite Volume based formulations has been presented for the elasto-plastic bending analysis of Mindlin-Reissner plates, where Von Mises yield criterion has been used. To expose the capability of the present approach in the elasto-plastic bending analysis of plates, the formulation has been utilized for the analysis of a series of plates with different boundary conditions. The results of the layered Finite Volume approach and ANSYS software results have been used for the comparison purposes. These comparisons have revealed that both methods predict almost the same nonlinear equilibrium paths for the cases considered. Although, their prediction of the stress resultants corresponding to the plate cross sections are nearly the same, but depending on the plate boundary conditions and loading types, in some cases, the non-layered model provides slightly higher estimations. Also, the non-layered approach is considerably faster, especially in plates with a large number of elements. Whatever the number of elements or number of layers increases, the difference between the simulation times of two methods goes up. So, if the speed of simulation is concerned, one may prefer the non-layered approach. It is worth mentioning that although the non-layered Finite Volume approach can provide comparable predictions for stress resultants in plate cross sections; however, it cannot provide information of how plasticity evolves over the plate thickness. On the other hand, the layered Finite Volume approach has the privilege of being able to provide information of plastic growth through the plate thickness.

REFERENCES

Aguirre, M., Gil, AJ., Bonet, J. and Lee, CH. (2015). "An upwind vertex centred Finite Volume solver for Lagrangian solid dynamics", *Journal of Computational Physics,* 300, 387-422.

Bailey, C. and Cross, M. (1995). "A Finite Volume procedure to solve elastic solid mechanics problems in three dimensions on an unstructured mesh", *International Journal for Numerical Methods in Engineering*, 38(10), 1757-1776.

Basic´, H., Demirdzˇic´, I. and Muzaferija, S. (2005). "Finite volume method for simulation of extrusion processes", *International Journal for Numerical Methods in Engineering,* 62(4), 475-494.

Bathe, K.J. (1996). *Finite Element procedures*, Prentice-Hall, New Jersey, USA.

Cardiff, P., Tuković, Ž., Jasak, H. and Ivanković, A. (2016). "A block-coupled Finite Volume methodology for linear elasticity and unstructured meshes", *Computers and Structures,* 175, 100-122.

Cardiff, P., Tuković, Ž., De Jaeger, P., Clancy, M. and Ivanković, A. (2017). "A lagrangian cell-centred Finite Volume method for metal forming simulation", *International Journal for Numerical Methods in Engineering,* 109(13), 1777-1803.

Cavalcante, M.A.A., Marques, S.P.C. and Pindera, M-J. (2011). "Transient Finite Volume analysis of a graded cylindrical shell under thermal shock loading", *Mechanics of Advanced Materials and Structures*, 18(1), 53-67.

Cavalcante, M.A.A., Pindera, M-J. and Khatam, H. (2012). "Finite-Volume micromechanics of periodic materials: Past, present and future", *Composites B*, 43(6), 2521-2543 .

Cavalcante, M.A.A. and Pindera, M-J. (2012). "Generalized Finite-Volume theory for elastic stress analysis in solid mechanics, Part I:

Framework", *Journal of Applied Mechanics*, 79(5), 051006-11.

Demirdzˇic´, I., Martinovic´, D. and Ivankovic´, A. (1988). "Numerical simulation of thermal deformation in welded workpiece", *Zavarivanje*, 31, 209-219, (in Croatian).

Demirdžić, I. and Martinović, D. (1993). "Finite volume method for thermo-elasto-plastic stress analysis", *Computer Methods in Applied Mechanics and Engineering*, 109(3-4), 331-349.

Edalati, H. and Soltani, B. (2015). "Analysis of thin isotropic and orthotropic plates with Element-Free Galerkin method and various geometric shapes", *Journal of Computational Methods in Engineering*, 34(2), 143-157.

Fallah, N. (2004). "A cell vertex and cell centred Finite Volume method for plate bending analysis", *Computer Methods in Applied Mechanics and Engineering*, 193(33-35), 3457-3470.

Fallah, N. (2006). "On the use of shape functions in the cell centered Finite Volume formulation for plate bending analysis based on Mindlin-Reissner plate theory", *Computers and Structures*, 84(26-27), 1664-1672.

Fallah, N. and Parayandeh-Shahrestany, A. (2014). "A novel Finite Volume based formulation for the elasto-plastic analysis of plates", *Thin-Walled Structure*, 77, 153-164.

Ghannadiasl, A. and Noorzad, A. (2016). "Bending solution for simply supported annular plates using the Indirect Trefftz Boundary method", *Civil Engineering Infrastructures Journal*, 49(1), 127-138.

Harrison, D., Ward, T.J.W. and Whiteman, J.R. (1984). "Finite Element analysis of plates with nonlinear properties", *Computer Methods in Applied Mechanics and Engineering*, 34(1-3), 1019-1034.

Hughes, T.J.R., Cohen, M. and Haroun, M. (1978). "Reduced and selective integration techniques in the Finite Element analysis of plates", *Nuclear Engineering and design*, 46(1), 203-222.

Ivankovic, A., Demirdzic, I., Williams, J.G. and Leevers, P.S. (1994). "Application of the Finite Volume method to the analysis of dynamic fracture problems", *International Journal of Fracture*, 66 (4), 357-371 .

Kim, S.E., Thai, H.T. and Lee, J. (2009). "Buckling analysis of plates using the two variable refined plate theory", *Thin-Walled Structures*, 47(4), 455-462.

Liu, G.R. (2010). *Meshfree methods: Moving beyond the Finite Element method second edition*, CRC Press, New York, USA.

Mikaeeli, S. and Behjat, Ba. (2016). "3-D bending analysis of thick functionally graded plate in different boundary conditions using Element-Free Galerkin (EFG) method", *Journal of Solid and Fluid Mechanics*, 6(2), 109-120.

Mirzaei, S., Azhari, M. and Rahim, S.H. (2015). "On the use of finite strip method for buckling analysis of moderately thick plate by refined plate theory and using new types of functions", *Latin American Journal of Solids and Structures*, 12(3), 561-582.

Mirzapour, A., Eskandari Ghadi, M. and Ardeshir-Behrestaghi, A. (2012). "Analysis of transversely isotropic half-spaces under the effect of bending of a rigid circular plate", *Civil Engineering Infrastructures Journal*, 45(5), 601-610.

Naderi, A. and Baradaran, G.H. (2013). "Element free Galerkin method for static analysis of thin micro/nanoscale plates based on the nonlocal plate theory", *International Journal of Engineering*, 26(7), 795-806.

Nordbotten, J.M. (2014). "Cell-centered Finite Volume discretizations for deformable porous media", *International Journal for Numerical Methods in Engineering*, 100(9), 399-418.

Osadebe, N. N. and Aginam, C. H. (2011). "Bending analysis of isotropic rectangular plate with all edges clamped: Variational symbolic solution", *Journal of Emerging Trends in Engineering and Applied Sciences*, 2(5), 846-852.

Owen, D.R.J. and Hinton, E. (1980). *Finite Elements in plasticity: Theory and practice*, Pineridge Press, UK.

Prathap, G. and Bhashyam, G.R. (1982). "Reduced integration and the shear-flexible beam element", *International Journal for Numerical Methods in Engineering*, 18(2), 195-210.

Reddy, J.N. (2004). *Mechanics of laminated composite plates and shells: Theory and analysis*, CRC Press, Boca Raton, FL, Second Edition.

Reissner, E. (1945). "The effect of transverse shear deformation on the bending of elastic plates", *ASME Journal of Applied Mechanics*, 12, 69-77.

Rezaiee-Pajand, M. and Sadeghi**,** Y. (2013). "A bending element for isotropic, multilayered and piezoelectric plates", *Latin American Journal of Solids and Structures*, 10(2), 323-348.

Ruocco, E. and Fraldi, M. (2012). "An analytical model for the buckling of plates under mixed boundary conditions", *Engineering Structures*, 38, 78–88.

Shahabian, F., Elachachi, S.M. and Breysse, D. (2013). "Safety analysis of the patch load resistance of plate girders: Influence of model error and variability", *Civil Engineering Infrastructures Journal*, 46(2), 145-160.

Shi, G. and Voyiadjis, G.Z. (1992). "A simple non-layered Finite Element for the elasto-plastic analysis of shear flexible plates", *International*

Journal for Numerical Methods in Engineering, 33(1), 85-99.

Stylianou, V. and Ivankovic, A. (2002). "Finite Volume analysis of dynamic fracture phenomena", *International Journal of Fracture*, 113(2), 107-123.

Sudhir, N. (2012). "Plate bending analysis using Finite Element method", Bachelor Thesis, Deemed University.

Tang, T., Hededal, O. and Cardiff, P. (2015). "On Finite Volume method implementation of poro-elasto-plasticity soil model", *International Journal for Numerical and Analytical Methods in Geomechanics,* 39(13), 1410-1430.

Timoshenko, S.P. and Woinowsky-Krieger, S. (1970). *Theory of plates and shells,* McGraw-Hill, New York.

Trangenstein, JA. (1991). "The riemann problem for longitudinal motion in an elastic-plastic bar", *SIAM Journal on Scientific and Statistical Computing,* 12(1), 180-207.

Wheel, M.A. (1997). "A Finite Volume method for analyzing the bending deformation of thick and thin plates", *Computer Methods in Applied Mechanics and Engineering,* 147(1-2), 199-208.

Xia, P., Long, S.Y. and Wei, K.X. (2011). "An analysis for the elasto-plastic problem of the moderately thick plate using the meshless local Petrov Galerkin method", *Engineering Analysis with Boundary Elements,* 35(7), 908-914.

Xu, Y. P. and Zhou, D. (2010). "Three-dimensional elasticity solution of transversely isotropic rectangular plates with variable thickness", *Iranian Journal of Science and Technology,* 34(B4), 353-369.